Applied Catalysis B: Environmental 202 (2017) 269–280

Contents lists available at ScienceDirect

Applied Catalysis B: Environmental

journal homepage: www.elsevier.com/locate/apcatb

Oxidation of furfural in aqueous H_2O_2 catalysed by titanium silicalite: Deactivation processes and role of extraframework Ti oxides

A.C. Alba-Rubio[a,1], J.L.G. Fierro[b], L. León-Reina[c], R. Mariscal[b], J.A. Dumesic[a], M. López Granados[b,*]

[a] Department of Chemical and Biological Engineering, University of Wisconsin-Madison, 1415 Engineering Drive, Madison, WI, United States
[b] Instituto de Catálisis y Petroleoquímica (CSIC), C/Marie Curie, Campus de Cantoblanco, E-28049 Madrid, Spain
[c] Servicios Centrales de Apoyo a la Investigación, SCAI, Universidad de Málaga, Campus Teatinos s/n, 29071 Málaga, Spain

ARTICLE INFO

Article history:
Received 14 July 2016
Received in revised form 6 September 2016
Accepted 13 September 2016
Available online 13 September 2016

Keywords:
Furfural
Maleic acid
Oxidation
Liquid phase
Hydrogen peroxide

ABSTRACT

Titanium silicalites (TS-1) with different Ti/Si atomic ratio (0.01–0.08) have been prepared, characterised by different techniques (X-Ray Diffraction, Transmission Electron Microscopy and Raman, Diffuse Reflection Infrared Fourier Transform and X-Ray Photoelectron spectroscopies), and their catalytic properties were investigated for the liquid phase oxidation of furfural with aqueous H_2O_2. For samples prepared with an initial Ti/Si > 0.01, extraframework Ti oxide is present and become more important as Ti loading increases. Two types of extraframework Ti have been identified: (i) anatase Ti oxide located at the external surface of zeolite crystals and (ii) Ti oxide nanodomains occluded within the channels and cavities of the zeolite. The latter can block the access of reactants to the active framework Ti(IV) sites for samples prepared with an initial Ti/Si > 0.04 and their removal results in an improvement in the selective oxidation of furfural to valuable products. Fouling by deposition of heavy by-products and Ti leaching were identified as two main causes of catalyst deactivation. The former can be reverted by removal of the deposits through calcination under air at 773 K. Leaching affects both the extraframework Ti and the active framework Ti species. During the first runs of reutilization, the Ti leaching is severe, affecting mainly to extraframework Ti oxide. Initially this leaching may be positive because its removal leads to the elimination of species blocking the access of reactants to the active Ti species; but in the longer term, the continuous leaching of active framework Ti irreversibly deactivates the catalyst.

1. Introduction

Maleic anhydride (MA) and its derived product maleic acid (MAc) are petrochemicals currently obtained by oxidation of, mostly, butane [1,2] with multiple applications in the current industry, ranging from the production of unsaturated polyesters resins, vinyl copolymers, agrochemicals, pharmaceuticals, food additives, etc. Recently there has been research directed at developing new renewable routes to produce some of these two commodities by oxidation of biomass-derived platforms like butanol [3], levulinic acid [4], hydroxymethylfurfural [5] and furfural [6–13]. MA and MAc can be interconverted into each other, and therefore the production of one of them implies the availability of the other.

The furfural route seems appealing, because furfural is currently a renewable commodity produced from lignocellulosic agroresidues with an annual rate of ca. 300 Kton [14,15]. Furfural already presents several commercial applications and, besides, other transformations to biofuels, commodities and fine chemicals have been technically demonstrated [16–18]. Accordingly, furfural has been pointed as one of the top value-added chemicals derivable from biomass [19].

Furfural oxidation can be accomplished either in gas phase [6] or in liquid phase [17]. The latter is conducted at lower temperatures (303–343 K), which may be crucial when considering a commercial application. Modest yields have been accomplished by using O_2 as oxidant [7,8,10]; the latter presents also the drawback of requiring high O_2 pressure (1–2 MPa). To the best of our knowledge, the highest yield of MAc (close to 80%) has been obtained using hydrogen peroxide as oxidant and titanium silicalite (TS-1) as catalyst [9]. Other catalysts have also been tested in the oxidation with

* Corresponding author.
E-mail address: mlgranados@icp.csic.es (M. López Granados).
[1] Present address: Department of Chemical and Environmental Engineering, University of Toledo, Toledo, OH 43606, United States.

http://dx.doi.org/10.1016/j.apcatb.2016.09.025
0926-3373/

hydrogen peroxide, possessing strong Brønsted acid sites like sulfonic groups [11,12]. In such cases, there is a lack of selectivity of MAc because a wide range of C4 dicarboxylic acids like succinic, fumaric, malic and tartaric acids are formed with significant yields, especially succinic acid. The reason for the high MAc yield found with TS-1 seems to be related to the different mechanism through which the reaction proceeds. A route involving hydroxy-furan-2(5H)-one (HFONE) as an intermediate is selectively preferred in the case of TS-1 (see Scheme 1 for the mechanism proposed elsewhere [9]), whereas in the case of catalysts having sulfonic groups two different routes are possible, one affording succinic acid and the other one yielding MAc and its derived acids [9,11,12].

It has been proposed that TS-1 is selective for this reaction because of the presence of isolated tetrahedral sites incorporated to the silicalite framework [9,20,21]. The first step of the reaction has been proposed to be the epoxidation of one of the double bonds of the furan ring and the substitutional Ti atoms are well known to be active in this epoxidation reaction [22]. Besides these tetrahedral Ti sites, extraframework octahedral Ti sites in anatase-like domains TiO_2 can be also present in TS-1, and actually they were present in the commercial TS-1 used in previous research [9]. In principle these extraframework Ti species should not be involved in the epoxidation reaction but it must bear in mind that the formation of HFONE and MAc requires other reactions different to epoxidation of double bonds and therefore it is not clear whether the octahedral extraframework Ti species in anatase can be involved in those further steps, whether they are just spectator species, or even whether they have an undesirable effect on the reaction of oxidation of furfural to MAc. Thus, within this context, a synergy between the framework Ti species and the anatase type extra-framework titanium has already been invoked to explain the outstanding catalytic performance of TS-1 in styrene epoxidation [23].

The maximum amount of Ti that can be efficiently incorporated in the silicalite framework is equivalent to a Ti/Ti + Si atomic ratio of around 0.025 [24]. Using a larger ratio in the synthesis does not result in proportional incorporation of more Ti in the framework, but leads to the formation of extraframework anatase Ti oxide. In this work, a series of TS-1 samples has been prepared by a conventional methodology increasing the Ti initially present in the preparation vessel from a low amount of Ti to that exceeding the Ti that can be effectively incorporated to the framework. In this way, a set of samples with anatase concentration ranging from traces of anatase to high concentration of anatase was prepared. Thus the role of the presence of extraframework Ti oxide in the chemical and catalytic properties can be investigated. To deeper probe the role of extraframework TiO_2, the effect of removing anatase Ti oxide by washing with aqueous HCl both on the chemical and catalytic properties was also conducted.

Regarding the reusability properties of the catalyst, no deactivation was observed in the stability investigation previously conducted using high grade furfural, despite the fact that deactivation of TS-1 by fouling is a common phenomenon found in the epoxidation of other molecules [25–27] and that leaching of both Ti species was observed upon reutilization [9]. In this previous study, the reutilization tests were conducted after 24 h of reaction. At such long time of reaction, the conversion and the yield of the relevant products are in an asymptotic regime, and deactivation could only have been detected if it were extensive [28]. In an attempt to reveal the deactivation processes with low-medium impact, in the present article the reutilization tests were conducted under conditions giving rise to lower conversion and yields. Furthermore, more reutilization runs than in previous study were conducted to assess the longer term stability of the system.

2. Experimental

2.1. Materials and preparation of titanium silicalites with different Ti/Si at. ratios

Different TS-1 samples were prepared by following the procedure described elsewhere [29] by using tetraethyl orthosilicate (TEOS) and tetraethyl orthotitanate (TEOT) as sources of Si and Ti, respectively (supplied by Sigma Aldrich). TEOT was dropwise incorporated to a flask containing the corresponding TEOS at 308 K. Addition was done under stirring and N_2 atmosphere. After 30 min of stirring, the solution flask was chilled by an ice bath and then an 1 M aqueous solution of tetrapropylammonium hydroxide (TPAOH) was added to the solution. Initially the addition was slow (less than 1 drop min^{-1}). After 1 h, the addition rate was successively increased. Once the TPAOH addition was ended, 10 mL of H_2O were incorporated to the synthesis flask and left under stirring overnight at room temperature. Subsequently, the synthesis mixture was heated at 323 K for 4 h. Ethanol and H_2O can be evaporated during this period of agitation, the volume of the solution was kept constant by repeated additions of more H_2O. A flowing stream of

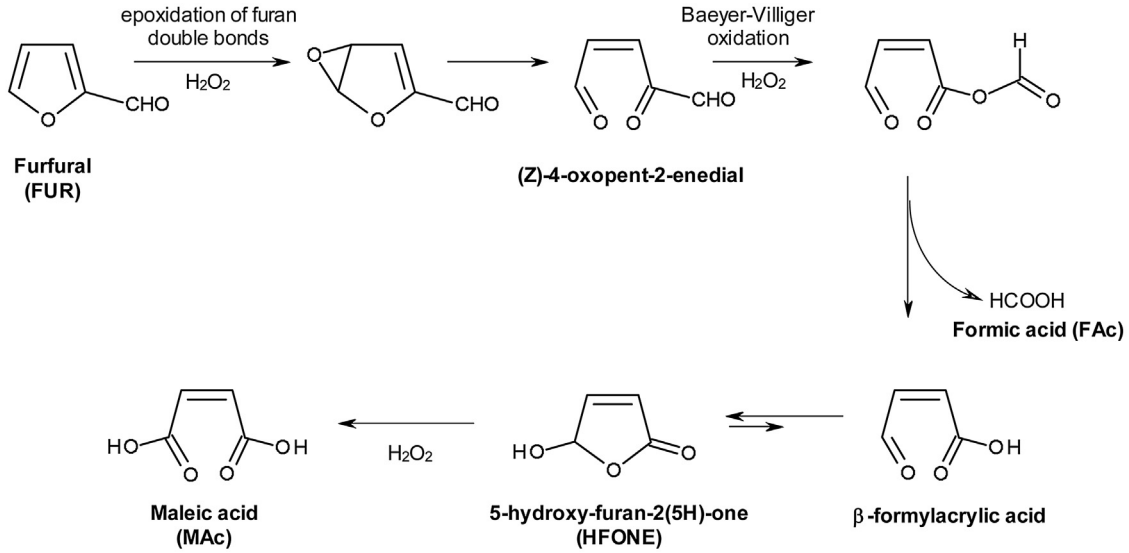

Scheme 1. Route of formation of Maleic acid via 2-hydroxy-furan-2(5H)-one.

N_2 was maintained throughput these initial steps of formation of the sol.

The former solution was then transferred to a Teflon-lined autoclave and heated to 443 K for 4 h. The formed solid was subjected to several cycles of centrifugation and rinsing with deionized water until neutral pH of the rinsing water. The solid was then dried at 393 K for 2 h (heating ramp 0.030 K min^{-1}) and then calcined at 623 K for 10 h (heating ramp 0.083 K min^{-1}).

Five solids were prepared by changing the amounts of TEOS, TEOT, TPAOH and H_2O used for the synthesis as to have mol ratio of SiO_2:TiO_2:TPAOH:H_2O equal to 1:x:0.3:18; where x = 0, 0.01, 0.02, 0.04 and 0.08. The solid with x = 0 is a Ti-free silicalite. The Ti/Si ratio was changed from a low amount of Ti to that exceeding the Ti that can be effectively incorporated to the framework. These as-prepared solids were labelled as TS0.0x.

For comparison purposes a commercial titanium silicalite-1 with a Ti/Si at. ratio of 0.039 (TXRF analysis) [9] and purchased from Tricat Zeolites was also investigated and named as TScom.

2.2. Washing of the as-prepared samples with HCl

The as-prepared solids were washed with 1 M HCl solution (50 mL of HCl solution g^{-1} of solid) for 24 h under stirring. The solid was subsequently subjected to several cycles of centrifugation and rinsing with deionized water until neutral pH of the rinsing water. Then the solid was dried and calcined following the procedure described above. The samples were labeled as TS0.0x-HCl.

2.3. Characterisation of the samples

TXRF (total reflection X-ray fluorescence) analysis of solids was performed in a S2 PICOFOX instrument equipped with two X-ray fine focus lines, Mo and W anodes, and a Co(Li) detector with an active area of 80 mm^2 and a resolution of 157 eV at 5.9 keV (Mn Kα). The acquisition time was 300 s and 500 s for qualitative and quantitative analysis, respectively. To carry out the TXRF analysis, a Mo X-ray source was used for Si and Ti determination. For the analysis of solid samples, 10–15 mg of sample was ground in an agate mortar to a powder with a particle size less than 10 μm. Subsequently, 10 mL of high-purity water was added to the powder. The sample was homogenised for 15–20 min by ultrasonic desagregation to disperse any possible agglomeration of particles. A 5-μL aliquot of the suspension was removed and placed on a flat carrier of plastic after which the water was evaporated by vacuum.

X-Ray diffraction patterns of the samples treated at 823 K were recorded on a PANalytical X'Pert PRO MPD diffractometer working in reflection geometry (θ/2θ) and using the X'Celerator RTMS (Real Time Multiple Strip) detector with an active length of 2.122°. The samples were loaded in a HTK1200 chamber from Anton Paar. The patterns were collected at 393 K (after cooling from 823 K) with a long fine focus Cu tube working at 45 kV and 40 mA. The incident beam optic path contained a primary monochromator which yielded a strictly monochromatic, λ = 1.54059 Å radiation. A typical scan range was used, measuring from 4.0 to 90.0° 2θ with a step size of 0.0167° 2θ and an overall recording time of approximately 3 h. The patterns were analyzed by the Rietveld method [30] using the GSAS program [31]. Only the overall parameters, histogram scale factor, background coefficients, unit cell parameters, zero-shift error and peak shape coefficients, were refined.

Raman spectra were recorded on a single-monochromator Renishaw 1000 spectrophotometer equipped with a CCD cool detector (200 K), with an argon laser as the excitation source (λ = 532 nm), a single monochromator, a supernotch filter, and an *in situ* cell that enables sample treatment under a flow of gas. Raman spectra were recorded at room temperature with a laser power of 2 mW after an *in situ* calcination of the samples in synthetic air with a heating rate of 10 K min^{-1} up to 833 K for 30 min.

Transmission electron microscopy (TEM) images were taken in a Tecnai TF-30 microscope operated at 300 kV with resolution of 2.3 Å. Electron energy loss spectroscopy (EELS) elemental maps were acquired at the same equipment by using a GIF Quantum energy filter system (EELS resolution 0.9 eV). Samples were first suspended in ethanol, ultrasonicated for 5 min and deposited onto carbon coated copper TEM grids.

X-ray photoelectron spectra (XPS) were acquired with a VG Escalab 200 R spectrometer equipped with a hemispherical electron analyser and a Mg Kα (1253.6 eV) X-ray source. The solids were outgassed at 393 K for 1 h at 10^{-5} mbar to remove water before transfer to the ion-pumped analysis chamber. Si 2p and Ti 2p spectra were scanned a sufficient number of times to obtain high signal-to-noise ratios (around 10 and 40–60 accumulations for Si 2p and Ti 2p core levels, respectively). The static charge of the samples was corrected by referencing binding energies (BEs) to the Si 2p peak (103.4 eV). The areas of the peaks were computed by fitting the experimental spectra to Gaussian/Lorentzian curves after removing the background (using the Shirley function). Surface atom ratios were calculated from peak area ratios normalised by using the corresponding atomic sensitivity factors [32].

The Diffuse Reflectance Infrared Fourier Transform (DRIFT) spectra were collected with a Nicolet 5700 spectrometer equipped with a Hg-Cd-Te cryodetector of high sensitivity, working in the spectral range of 4000–650 cm^{-1}. A Praying Mantis (Harrick Co) was used as mirror optical accessory. About 30 mg of samples, previously ground, were placed in a reaction camera that allows *in situ* thermal treatments (Harrick Scientific Products, NY). The device is equipped with a temperature controller and a gas mixing system (PID Eng & Tech) that allows the treatment of the samples under controlled atmosphere. Prior to the adsorption of deuterated acetonitrile, the surface of the samples was cleaned by heating with a 20 v/v% O_2/Ar flow while at 573 K for 1 h. Afterwards, the temperature was decreased to 25 °C in flow of Ar. Then this flow of Ar was bubbled through deuterated acetonitrile and contacted the solid for 20 min. Subsequently the feed was switched to only Ar flow and sample heated at 323 K for 15 min to remove physically adsorbed CD_3CN. DRIFT spectra of deuterated acetonitrile chemisorbed over the surface sites were then recorded with a resolution of 4 cm^{-1}. A KBr spectrum was selected as reference spectrum.

2.4. Catalytic activity and reutilization runs

The oxidation of furfural was carried out in an Ace glass reactor (15 mL). The required amounts of solid, furfural and H_2O_2 solution were loaded into the reactor. The reaction started when the reactor was immersed in a silicone oil bath set at the selected temperature. The reaction mixture was stirred by a magnetic bar at 800 rpm. After a given time, the reactor was taken out from the oil bath and its composition analyzed by HPLC as follows. A known amount of reaction mixture (ca. 0.25 g) was sampled and a known amount (ca. 0.25 g) of a 30 mg/g aqueous solution of oxalic acid and of deionized water (ca. 5 g) were added to it (oxalic acid was used as an internal standard). This diluted aliquot, after being filtered through a 0.22 μm syringe filter, was then analysed in an Agilent 1200 HPLC chromatograph equipped with a refraction index detector, and a Bio-Rad Aminex HPX-87H column (300 mm × 7.8 mm). A 0.005 M H_2SO_4 mobile phase was employed as the eluent at 328 K and a 0.4 mL/min flow rate. More details are given elsewhere [9].

Furfural conversion and product yields were calculated according to the following formulas:

$$\text{Furfural conversion (mol\%)} = \frac{m^0{}_{furf} - m_{furf}}{m^0{}_{furf}} \times 100$$

Table 1
Chemical analysis by TXRF (bulk) and XPS (surface) of as-prepared samples.

Sample	TXRF results			XPS results		
	at. Ti/Si	wt.% of Ti as TiO_2	wt.% K_2O	Ti $2p_{3/2}$		Ti/Si at. ratio
TS0.00	–	–	0.48	–		–
TS0.01	0.011	1.45 (1.31)[a]	0.51	458.0 (47%)[b]	0.031	Ti oct. 0.015
				459.5 (53%)[b]		Ti tetr. 0.016
TS0.02	0.022	2.83 (2.58)[a]	0.63	458.0 (75%)[b]	0.063	Ti oct. 0.047
				459.7 (25%)[b]		Ti tetr. 0.016
TS0.04	0.038	4.80 (5.06)[a]	0.60	458.2 (77%)[b]	0.089	Ti oct. 0.069
				459.4 (23 %)[b]		Ti tetr. 0.020
TS0.08	0.081	9.66 (9.58)[a]	0.95	458.4 (100%)[b]	0.301	Ti oct. 0.301

[a] Value between brackets are the nominal value (deduced from the Ti and Si precursor present in the preparation flask).
[b] Value between brackets represent the % of the area of each XPS peak.

$$\text{Product yield (mol\%)} = \frac{m_{prod}}{m^0_{furf}} \times 100$$

where m^0_{furf} refers to the mole quantity initially loaded into the reactor, and m_{furf} and m_{prod} refer to the number of moles of the furfural and products, respectively, in the reaction mixture at a given time. The HPLC chromatographic factor of the organic products was calculated by analysing solutions with known concentrations of the different organic products. The hydrogen peroxide concentration at a given reaction time was determined by iodometric titration. Further details of the protocol can be found elsewhere [9].

For catalyst reutilisation tests, a series of successive runs were conducted. After a given run the reaction mixture was centrifuged within the reactor and the reaction mixture carefully taken out with a syringe with a long needle for HPLC and H_2O_2 analysis. The solid left in the reactor was then subjected to 5 more cycles of washing with ca. 5 mL of deionised water-centrifugation and finally dried within the reactor at 333 K overnight before performing a new reaction run.

3. Results and discussion

3.1. Characterization and catalytic activity of as-prepared TS-1 catalysts

Table 1 summarizes the results of chemical analyses conducted on the different samples. The first columns refer to TXRF analysis of the bulk of the solids whereas those at the right side of table concern the surface analysis by XPS. The TXRF analysis shows that most of the Ti added as TEOT ends up in the solid, because both the Ti/Si atomic ratio and the Ti wt% expressed as TiO_2 were close to the nominal values deduced from the amounts of TEOS and TEOT in the synthesis. This does not mean that Ti is fully incorporated in the framework, because, as is well known, the capacity of the silicalite to accommodate Ti in its framework is limited. Potasium was also detected and it comes from the K impurity present in the TPAOH used in the synthesis [29].

XRD diffractograms of the as-prepared samples are represented in Fig. 1A. The presence of single reflections at theta ca. 24.4 and ca. 29.4 for Ti containing samples instead of the two doublets present in Ti-free silicalite is an evidence of the incorporation of Ti within the framework of the silicalite (see arrows). This is consequence of the orthorrombic symmetry (Pnma space group) of the titanium silicalites in contrast to the monoclinic symmetry ($P2_1/n11$ space group) adopted by the Ti-free silicalite [33]. The Rietveld analysis was also conducted using the XRD patterns obtained after subjecting the different samples at 823 K under a N_2 flow stream for a couple of hours in an in-situ chamber. The lattice parameters obtained for the different samples are represented in Fig. 1B (error bars are smaller than the size of the square points used in the graph). The insertion of the Ti cations produces an expansion of the lattice due the higher size of the Ti(IV) cation with respect to that of Si(IV) cation: the more the amount of Ti incorporated to the framework, the greater the lattice parameters [24,34]. We have to bear in mind that a linear correlation between the Ti/Si used for the synthesis and the lattice parameters is only expected for samples with Ti/Si at. ratio <0.025, provided that the preparation proceeds with the complete incorporation of Ti within the framework [24,34]. In our case, the lattice for sample TS0.01 has rapidly expanded with respect to TS0.00. Beyond this point using greater concentration of Ti during the synthesis does not result in a proportional incorporation of more Ti. Thus for TS0.02 sample the lattice parameters are quite similar to that of TS0.01, the TS0.04 lattice parameters are not four times greater than those of TS0.01 sample and those of TS0.08 sample are quite similar, although slightly larger, than that of TS0.04 sample. This means that, with the experimental set up here used for the preparation, for samples prepared with Ti/Si > 0.01 most of the Ti used in the synthesis does not end up incorporated into the silicalite structure but very likely as Ti oxide.

Fig. 2 represents the Raman spectra of the different as-prepared samples in the region between 100 and 250 cm^{-1}. This region was selected because anatase TiO_2 presents an intense band at around 145 cm^{-1} [9]. The Raman study demonstrates that for those samples with nominal at. Ti/Si ≥ 0.02, anatase-like domains are present in the solids. The size of these crystallites must be quite small because XRD failed to detect the presence of anatase.

The as-prepared samples were also studied by TEM (Fig. 3). The crystal size of the TS-1 is that expected taking into account the SiO_2:TiO_2:TPAOH:H_2O mol ratio used in the synthesis. According to Van der Pol et al. [29] these mol ratios result in the formation of dice-like nanocrystals with sides of roughly few hundred nanometers (100–300 nm) long. This morphology is a desired feature for a catalyst because it favors the diffusion of reactants and products within the inner channels. Arrows draw the attention of the presence of structures over the surface of the crystals of TS-1. In some cases these structure take the shape of a layer covering the surface of these TS-1 nanoparticles. The EELS maps conducted on TS0.08 sample (Fig. 3) reveal that Ti is the main metal present in the these surface nanostructures, strongly suggesting that anatase is present over the surface of the TS-1 nanoparticles.

Fig. 4A shows the Ti 2p core level for the different as-prepared catalysts (Fig. 4B will be later discussed when discussing the HCl-treated samples). The most relevant XPS information of as-prepared catalysts was included in Table 1. XPS is pertinent because it provides chemical information of the outermost region of the TS-1 nanoparticles. This information is complementary to that given by TXRF in Table 1. As seen in Fig. 4A, the Ti 2p core level for TS0.01, TS0.02 and TS-0.04 samples is wider than that of TS0.08 because these samples present two contributions; that at 458.2 ± 0.2 eV assigned to octahedral Ti and that at 459.5 ± 0.2 eV arising from tetrahedral Ti. The latter signal is assigned to Ti incorporated to the framework, whereas the former must correspond to Ti in Ti oxide

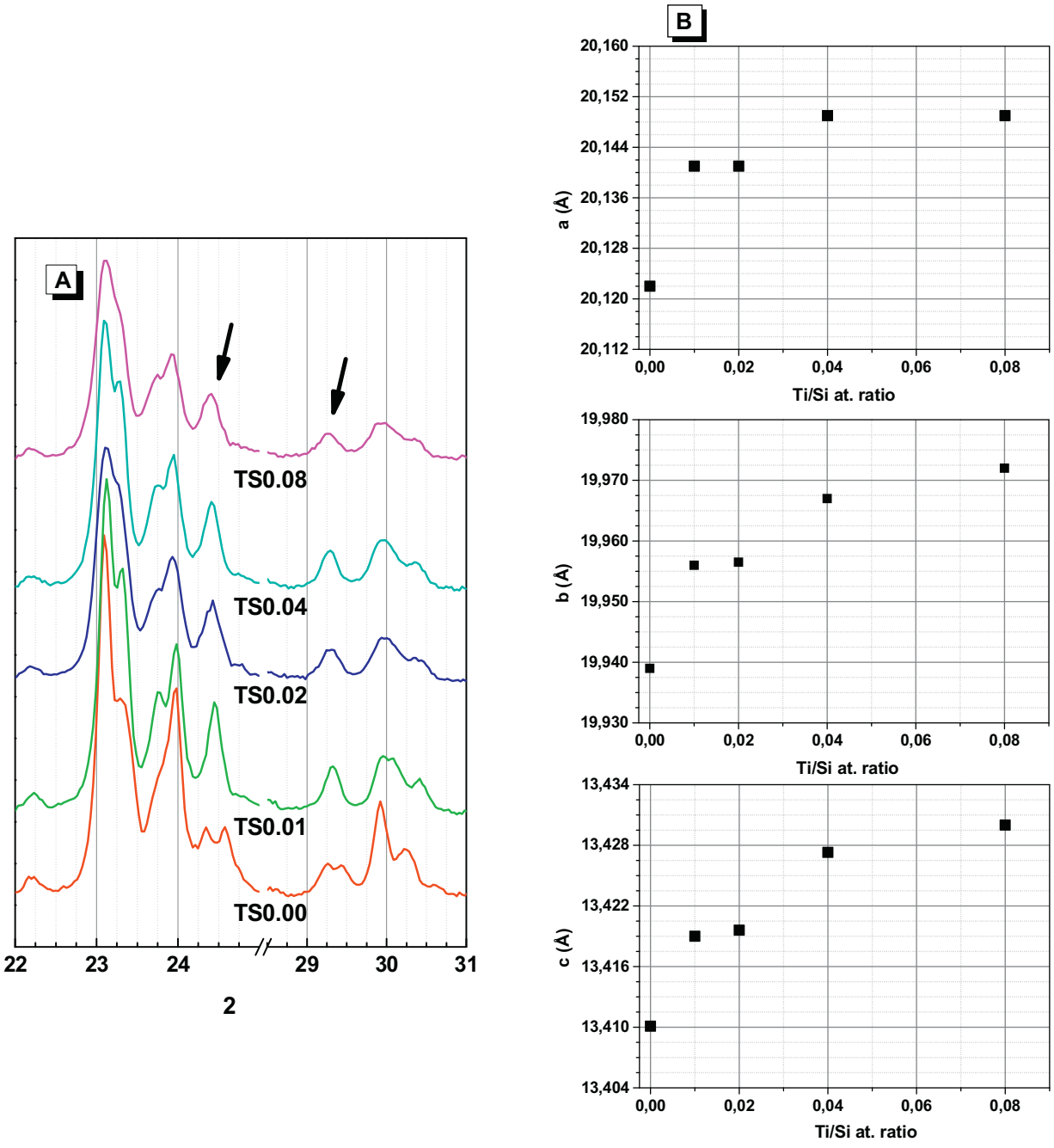

Fig. 1. XRD study of the as-prepared samples; a) XRD diffractograms and b) lattice parameters for the different samples as obtained by Rietveld analysis (see text for further details).

[9,22]. Octahedral Ti predominates in the TS0.02 and TS0.04 samples, representing ca. 75% of the Ti detected by XPS. The TS0.01 sample also presents the Ti in Ti oxide species, although Raman and XRD fail to detect it. On the other hand, the deconvolution of the Ti 2p core level of the TS0.08 sample requires only one contribution from octahedral Ti. Considering that Raman detect the presence of anatase over the surface of TS0.08 zeolite crystals, it can be assumed that the XPS octahedral signal arise mostly from surface anatase phase.

Another interesting conclusion regarding the location of Ti can be deduced from the XPS analysis. The results compiled in Table 1 also show that the XPS Ti/Si atomic ratios of the different samples are larger than those obtained from TXRF (bulk value). A closer look to the data shows that whereas the XPS Ti/Si atomic ratio of the tetrahedral species slightly increases relative to the nominal Ti/Si ratio, that of octahedral species experienced a more rapid increase. Therefore a significant fraction of the amount of Ti used in the synthesis ends up enriching the surface with octahedral Ti. This result is in agreement with the Raman and TEM results that showed that Ti oxide nanocrystallites are present over the surface of the TS-1 crystal. In addition, for the TS0.08 sample, this surface anatase must be extensively covering the surface of the zeolite, because the XPS signal from tetrahedral Ti could not be detected. In the ELSS map of Ti of TS0.08 sample a very thin layer of Ti oxide can be observed covering the surface of the TS-1 crystal.

Fig. 5 summarizes the catalytic properties of the different as-prepared TS-1 samples. Fig. 5A displays the kinetic curve of TS0.04 sample obtained when furfural is oxidized with aqueous H_2O_2

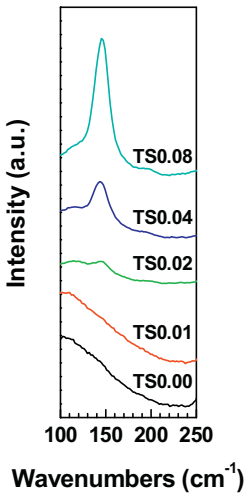

Fig. 2. Raman spectra of the different as-prepared samples in the 100–250 cm^{-1} region.

at 323 K, 5 wt% of catalyst and 5 wt% of furfural, and H_2O_2/FUR mol ratio of 2.5. Hydroxyfuranone (HFONE), MAc and formic acid (FAc) were the main products detected. Other products like fumaric acid (FumAc), malic acid (MalAc), tartaric acid (TarAc), furoic acid (FurAc) and furan-2(5H)-one were also observed, but each at yield lower than 5%, and they were not included in the figure for the sake of clarity. It must be stressed that the yield of FAc represented in Fig. 5 refers to that formed by total oxidation of furfural. One molecule of FAc is also formed for each of the C4 products mentioned above [9,35] and must be subtracted to calculate the yield of MAc formed by total oxidation. The carbon balance was around 60–70% throughout the reaction kinetics experiment. A plausible explanation for the lack of carbon balance will be given below.

HFONE is rapidly formed and it is the product with the highest yield. Furfural is fully converted after 8 h; H_2O_2 is then almost exhausted as conversion was close to 90% and consequently, beyond this time of reaction the rate of formation of other oxidation products from HFONE like MAc (and FumAc, MalAc, TarAc, etc) is depleted and their yield progresses slowly. The stoichiometric amount of H_2O_2 needed to form MAc is 3 whereas that of HFONE is 2; the latter is close to that used in the experiments of Fig. 5. A larger H_2O_2 concentration is required to form more MAc by oxidation of HFONE as demonstrated elsewhere [9].

Fig. 5B represents the catalytic behavior of the different as-prepared samples. The reaction conditions were 323 K, H_2O_2/FUR mol ratio = 2.5 and 4 h of reaction time. These conditions were selected to facilitate the detection of the deactivation of the catalyst upon reusing. At larger H_2O_2 concentration and longer time of reaction, the conversion would have been complete and the yield of the different products would have been in the asymptotic regime. When reusing the catalyst, if the conversion and yield of products were in the asymptotic regime, only extensive deactivation processes could be detected, whereas moderate deactivation processes may be unnoticed [28]. Another reason to use these conditions is that they favor the formation of HFONE. It has been previously reported that the formation of MAc from HFONE on TS-1 requires an excess of H_2O_2 and proceeds with inefficient consumption of H_2O_2 [9]. The efficiency of the process can be improved if a two-step process is implemented. TS-1 is first used with a H_2O_2/FUR mol ratio = 2 and once HFONE is formed a different catalyst (sulfonic resin), more efficient in the utilization of H_2O_2, conducts the final oxidation of HFONE to MAc [9].

The Ti free catalyst presents a conversion close to 50%, but the overall yield to oxidized products is below 5%. The presence of Ti results in the formation of more HFONE, MAc and FAc. The conversion of furfural and H_2O_2 become larger as the nominal Ti/Si atomic ratio increases, and thus for the TS0.08 sample, furfural and H_2O_2 conversions are close to 90% after 4 h. It is worth noting that

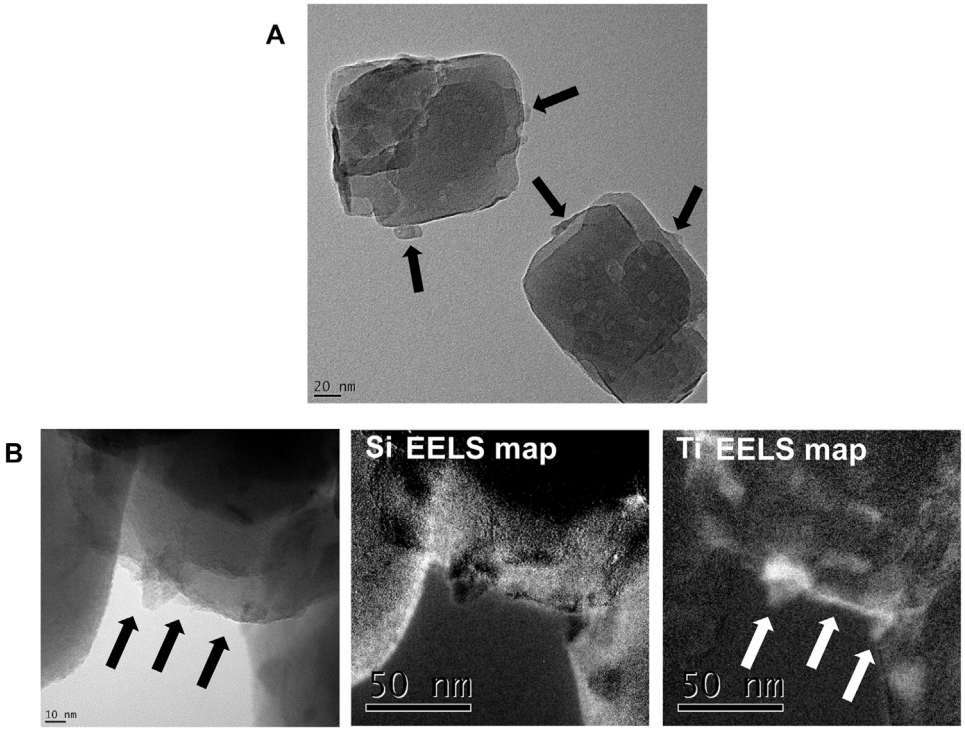

Fig. 3. Representative TEM micrographs of A) TS0.04 and B) TS0.08 samples. Aa a guide to the reader some of the surface anatase nanocrystallites are indicated by arrows. For TS0.08 sample the EELS elemental maps for Si and Ti are also included. The presence of those elements is revealed as white color in the corresponding EELS images.

Table 2
Chemical analysis by TXRF (bulk) and XPS (surface) of HCl-treated and used samples.

Sample	TXRF results			XPS results		
	at. Ti/Si	wt% TiO_2	wt% K_2O	Ti $2p_{3/2}$	Ti/Si at. ratio	
TS0.00-HCl	–	–	0.00	–		–
TS0.01-HCl	0.009	1.16	0.00	458.2 (23%)[a]	0.014	Ti oct. 0.003
				460.0 (77%)[a]		Ti tetr. 0.011
TS0.02-HCl	0.012	1.55	0.02	458.4 (33%)[a]	0.018	Ti oct. 0.006
				460.0 (67%)[a]		Ti tetr. 0.012
TS0.04-HCl	0.025	3.19	0.01	458.4 (73%)[a]	0.054	Ti oct. 0.040
				459.8 (27 %)[a]		Ti tetr. 0.014
TS0.08-HCl	0.047	5.84	0.02	458.6 (77%)[a]	0.137	Ti oct. 0.105
				460.0 (23%)[a]		Ti tetr. 0.032
TS-0.08-used	0.033	4.25	0	458.6 (43%)[a]	0.025	Ti oct. 0.011
				459.8 (57%)[a]		Ti tetr. 0.014
TS-0.08-used-calc	n.m.	n.m	n.m	458.3 (71%)[a]	0.029	Ti oct. 0.021
				460.1 (29%)[a]		Ti tetr. 0.008

n.m.: not measured.
[a] Value between brackets represent the % of the area of each XPS peak.

the furfural conversion and the yields of HFONE and MAc of TS0.08 are similar to those for the TS0.04 sample, but the H_2O_2 conversion of the former is greater than that of TS0.04 (90% vs. 50%). This comparison indicates that TS0.08 consumes H_2O_2 in an unselective manner. TScom catalyst is more active than TS0.04 and TS0.08 samples, the reason for this will be explained later when studying the removal of TiO_2 by HCl washing and especially when comparing the stability properties of TS0.08 and TScom.

The carbon balances for all of the catalysts at these reaction conditions were about 50–60%. It must be taken into account that at larger H_2O_2/Furfural ratios and/or longer reaction time the MAc yield and the C balance significantly improve (as we reported elsewhere [9]). Consequently the C imbalance is not mainly due to the deposition of unselective by-products; otherwise MAc yield could not have improved. It is also worth noticing that when there is no Ti in the silicalite (TS0.00 sample) the conversion is around 50% with the formation of very little products. There was also little conversion of H_2O_2, consequently the lack of C balance in this experiment can not be due to the formation of undetectable oxidised products. All these previous results strongly suggest that C imbalance is largely due to the adsorption of furfural over the internal and external surface of zeolite and not to the deposition of unselective products or the formation of undetectable products.

3.2. Effect of removal of Ti from TS-1 by the treatment with aqueous HCl

When the TS0.08 catalyst is in contact with the reaction mixture, the dissolution develops an intense orange-yellow color that strongly suggests that Ti oxide is dissolved by H_2O_2 forming yellow-orange colored Ti-peroxo complexes [36,37] (leaching will actually be confirmed below). Previous Raman, XPS and TEM resuts have showed that Ti oxide is present and extensively covering the surface of zeolite particles, especially of the TS0.08. All these aforementioned results motivated us to study the effect of removal of Ti oxide on the catalytic properties because such study conveys information of the role of Ti oxide in this reaction. The samples were the subjected to a treatment with aqueous HCl that has been shown to be very effective in dissolving Ti oxides [38]. The samples so obtained, HCl-treated samples, were characterized and their catalytic properties investigated.

Table 2 summarises the TXRF analysis of HCl-treated samples, and these results show that this treatment is effective in partly removing Ti from the as-prepared samples. Thus, the TXRF Ti/Si ratio goes from 0.012 in TS0.01 to 0.009 in TS-0.01-HCl (25% removal), from 0.022 to 0.012 (45% removal) in TS0.02, from 0.038 to 0.025 (34% removal) in TS0.04, and from 0.081 to 0.047 (42% removal) in TS0.08. The removal of K was also very effective.

XPS studies of HCl-treated samples were also conducted. Their spectra are represented in Fig. 4B, and the relevant XPS parameters are also included in Table 2. The decrease of the XPS Ti/Si ratio is even more pronounced than that detected by TXRF: 55, 66, 40 and 54% of removal, respectively. This removal affects both to the tetrahedral Ti and the octahedral Ti, but it is more intense for the octahedral Ti. This behavior is easily visible in the spectra of Fig. 4B: the contribution at around 459.9 ± 0.1 eV from tetrahedral Ti presents now higher relative intensity than in the as-prepared counterparts at the expense of the octahedral contribution. And for the TS0.08-HCl sample, this signal is now visible, whereas no tetrahedral contribution could be observed in the as-prepared TS0.08 sample. A more quantitative measure of the selective removal of the anatase Ti can be made by comparing the XPS Ti/Si atomic ratio of octahedral and tetrahedral Ti species between the as-prepared samples and the HCl-treated samples collected in Tables 1 and 2. Thus, for example, for TS0.02 the Ti tet/Si ratio goes from 0.016 to 0.012 (25% reduction) whereas that for Ti oct/Si goes from 0.047 to 0.006 (90% reduction).

Raman spectra of the washed samples were also recorded (Fig. S1 of the Supplementary content) and it was found that, despite the HCl-washing step, the band representative of anatase is still visible in the samples with Ti/Si ratio $\geq$0.02. TEM and EELS analysis were also conducted on TS0.08-HCl sample (Fig. S2) and Ti oxide (anatase) domains are clearly detected over the surface of the zeolite crystals. Since chemical analysis revealed that in all the samples a considerable fraction of the Ti oxide is removed by HCl-washing, especially at the surface, it appears that Ti oxide detected by TEM and located at the surface of zeolite crystals is not easily dissolved by the treatment. Consequently it seems likely that there is another Ti oxide species, more prone to be dissolved by HCl.

For a deeper understanding of the effect of the treatment with aqueous HCl, a DRIFT study of the chemisorption of deuterated acetonitrile (CD_3CN) was conducted (Fig. 6). This molecular probe is sensitive to the Ti incorporation in the zeolite framework, because Ti tetrahedral sites are Lewis acid sites and are susceptible of chemisorption of acetonitrile [39,40]. Acetonitrile chemisorbed on Lewis acids sites display a νCN vibration clearly distinguishable from that of acetonitrile chemisorbed on Brønsted acid sites. The interferences of Fermi resonances between the νCN and the $\delta_s(CH_3) + \nu$C-C combination in non-deuterated acetonitrile are absent in the deuterated probe and the corresponding spectrum is clearer and easier to assign the absorption bands. Fig. 6 collects the DRIFT spectra on different TS0.08 samples. The spectra of two reference samples, silicalite and pure anatase TiO_2, were

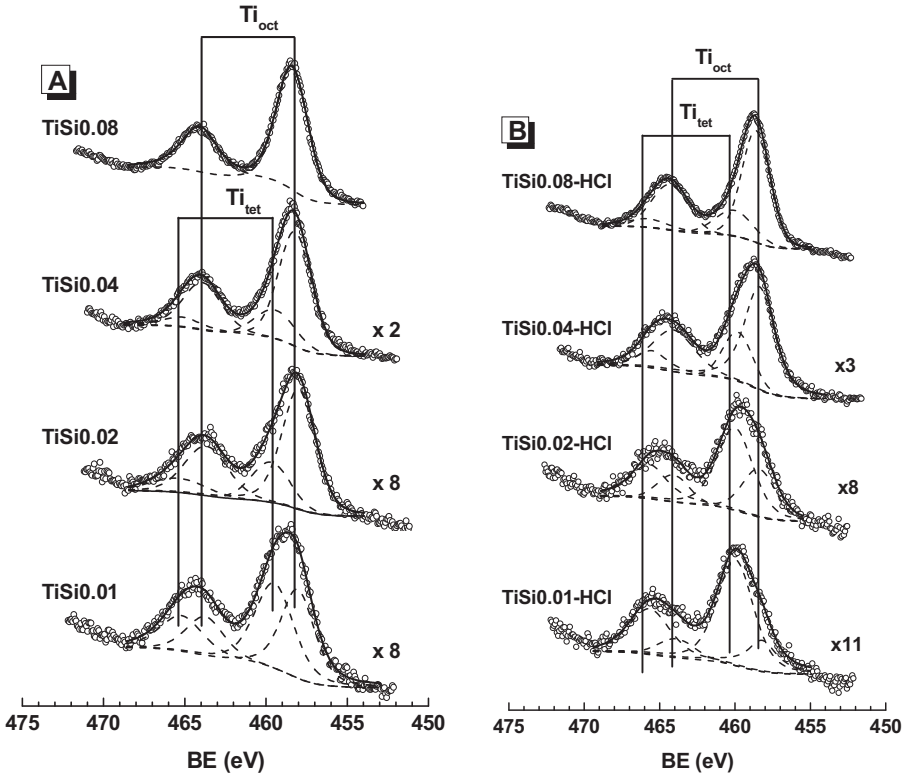

Fig. 4. Ti 2p core level of the (A) as-prepared samples and (B) HCl-treated samples.

also included for the sake of comparison. Regarding the spectra for the as-prepared TS0.08 sample, an intense band at 2270 cm^{-1} from acetonitrile chemisorbed on silanols groups (Brønsted acid sites) prevails over the weaker one on Lewis acid sites at 2300 cm^{-1}. This latter band is absent in the spectrum of the Ti-free silicalite. Fig. 6 also demonstrates that anatase can also present Lewis sites, but the corresponding acetonitrile DRIFT signal is much weaker and shifted to lower energy; therefore the signal at 2300 cm^{-1} is assigned to Ti(IV) incorporated to silicalite framework.

In the TS0.08-HCl sample the intensity of the band corresponding to the Lewis sites is similar to that from Brønsted acid sites. This behavior is consistent with the removal of Ti oxide domains that prevent the chemisorption of acetonitrile on the Ti(IV) sites. Once Ti oxide is extensively removed, the Lewis sites become accessible. One could possibly conclude that the anatase nanocrystals that have been detected by TEM and XPS covering the surface of the as-prepared TS0.08 catalyst may restrict the diffusion of acetonitrile into the channels and cages and consequently its chemisorption on the inner Lewis Ti(IV) sites. However this conclusion must be discarded. The intensity of the silanol-related band in the TS0.08 sample is similar to that in TS0.08-HCl sample, indicating that diffusion of deuterated acetonitrile within the channels and cages in TS0.08 sample is not restricted. Consequently, the low intensity of the 2300 cm^{-1} band in the as prepared TS0.08 must be due to

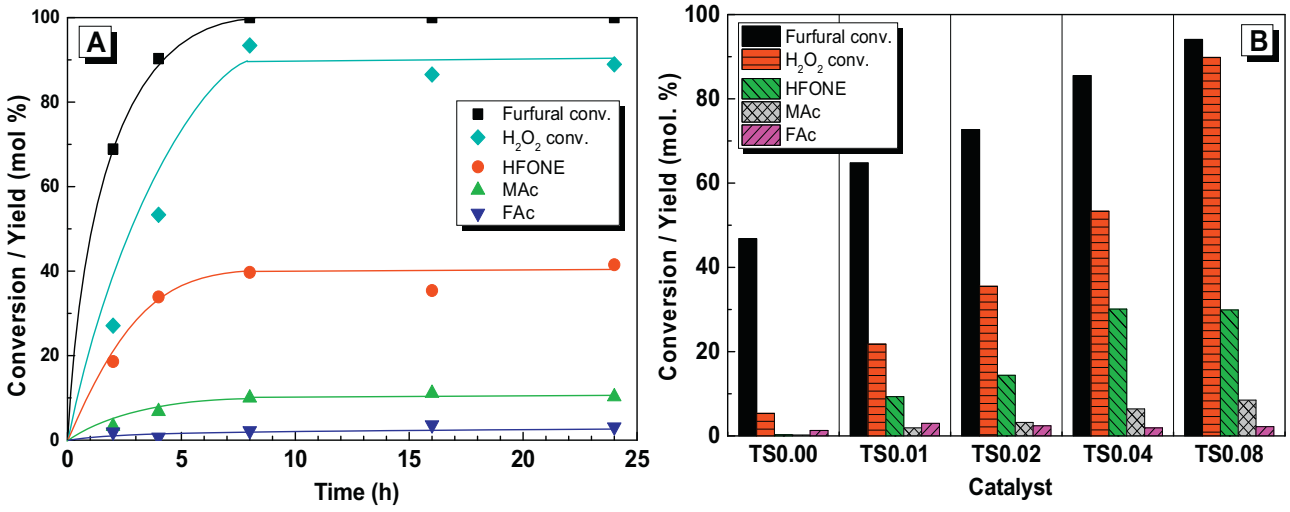

Fig. 5. Catalytic activity of different as-prepared samples. A) Kinetic curve of TS0.04 sample; B) comparison of the performance of the as-prepared different catalyst at 4 h of reaction time. Reaction conditions: 323 K, 5 wt% of catalyst, 5 wt% of furfural and H_2O_2/FUR mol ratio of 2.5.

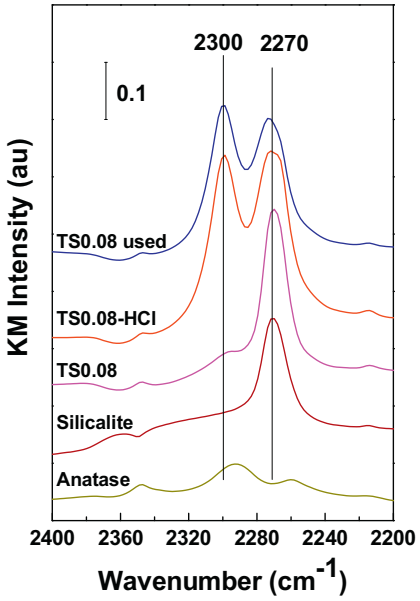

Fig. 6. DRIFT spectra of deuterated acetonitrile for different TS0.08 samples studied and reference samples.

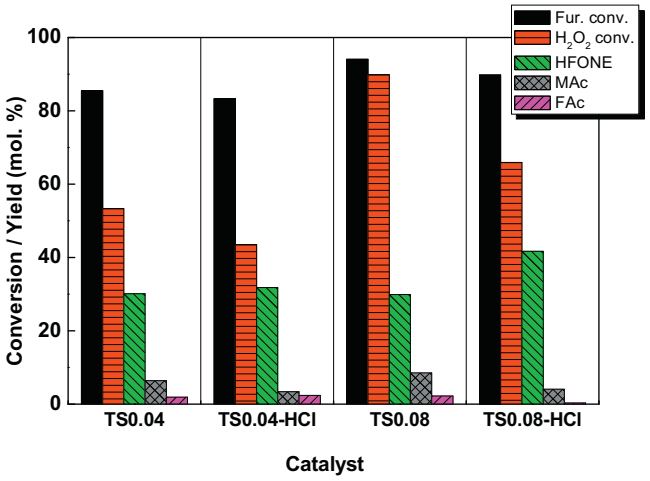

Fig. 7. Comparison of the performance of some of the HCl-treated catalyst at 4 h of reaction time, 323 K, 5 wt% of catalyst, 5 wt% of furfural and H_2O_2/FUR mol ratio of 2.5.

another reason: the presence of Ti oxide nanodomains within the channels and cavities of the zeolite in close contact with the substitutional tetrahedral Ti(IV) sites, selectively blocking the framework Ti(IV) Lewis sites and preventing the chemisoprtion.

It must be taken into account that, during the initial stages of the hydrothermal crystallization of TS-1, extraframework Ti oxide nanodomains with octahedral coordination are occluded within the channels and cavities of the early silicalite crystals [41]. In these premature crystals the content of tetrahedral Ti incorporated in the framework is low but as the hydrothermal crystallization progresses the occluded octahedral Ti extraframework species are incorporated to the framework [41]. Consequently, in TS0.08 sample it is expectable the presence of very small nanodomains of octahedral Ti oxide, occluding the pores and blocking the access of acetonitrile to tetrahedral Ti sites. We have to remember that in the TS0.08 sample a large excess of Ti was incorporated in the synthesis vessel, unable to be fully incorporated into the framework. Besides the occluded Ti oxide nanodomains, larger anatase nanostructures are present at the external surface of the zeolite crystals. The HCl-washing is much more efficient for the removal of the occluded Ti oxide nanodomains. The size of these nanodomains occluded within the channels must be smaller than that of the surface Ti oxide nanocrystals what explains its faster dissolution. On the contrary, the surface anatase nanocrystals detected by TEM studies are more recalcitrant to the HCl-treatment and, although it may undergo some leaching, they still remain after the washing treatment. Very likely very small anatase domains present at the surface have also been dissolved because XPS detects a substantial decrease of Ti after washing, but the larger anatase crystals remain.

All of the characterization data presented above point to a substantial removal of Ti oxide nanodomains occluded within the channels of the TS-1 when washing with aqueous HCl. This procedure does not remove all the octahedral species and, moreover, it also removes active tetrahedral species. The question is how does this HCl-treatment affect the catalytic properties? The Fig. 7 reveals the catalytic activity of TS0.04-HCl and TS0.08-HCl samples. For an easier comparison, the figure also includes the data of the as-prepared counterparts (already represented in Fig. 5). Importantly, the removal of Ti oxide by HCl-washing results in lower conversion of H_2O_2. This beneficial effect is more intense in the TS0.08-HCl. This more selective utilization of H_2O_2 is due to the removal of Ti oxide species by HCl (both the surface anatase nanocrystals and the occluded Ti oxide nanodomains) because it is well known that Ti oxide is involved in the unselective decomposition of H_2O_2 [22].

Regarding the furfural conversion, the treatment with HCl does not have any visible improvement effect, likely because we are in the asymptotic kinetic regime and the conversion is already high before the washing. It must be recalled that ca. 50% of the conversion is due to furfural retention by silicalite. The HCl-washing also results in better yield of HFONE, this effect is again more visible in TS0.08 sample than in TS0.04 sample. This effect is related to the presence of Ti oxide nanodomains occluded within the channels and cages and not to the anatase nanocrystals. DRIFT investigation indicated that although anatase particles are extensively covering the surface of the zeolite particles, they do not restrict the access to the channels and inner cavities. The Ti oxide nanodomains within the channels and cavities are responsible for the blocking of the active Ti(IV) sites. The better HFONE yields of TS0.08-HCl sample can be related to the removal of this occluded Ti oxide nanodomains: a better access of H_2O_2 to the selective tetrahedral framework Ti sites explains the enhanced HFONE yield. It seems reasonable that TS0.08 catalyst must present more Ti oxide occluded within the channels than TS0.04 because much more Ti was used in the synthesis. Consequently the effect of the removal of these species on the catalytic activity of TS0.04 is expected to be smaller. The possibility that the higher yield of HFONE is due to a higher availability of H_2O_2 in TS0.08-HCl can be discarded (this catalyst showed lower conversion of H_2O_2 and therefore there is more H_2O_2 available). The yield of HFONE in TS0.04 HCl is not that high and the availability of H_2O_2 is to that in TS0.08-HCl. Finally it is worth noticing that the MAc yield is lower for the HCl-treated samples. We will come back later to this undesirable effect when discussing below the reutilization properties.

Before going further it is important to realise that, considering all the previous results and the blocking effect that Ti oxide nanodomains has on the active Ti(IV) species, TS0.08 should have not been active. However, as it will be demonstrated below, the Ti oxide nanodomains are also dissolved by H_2O_2 in the course of the reaction. This leaching makes active the TS0.08 catalyst. HCl-treatment is more efficient in removing Ti oxide than the leaching by H_2O_2 occurring in the course of the reaction and consequently TS0.08-HCl catalyst is most selective to HFONE.

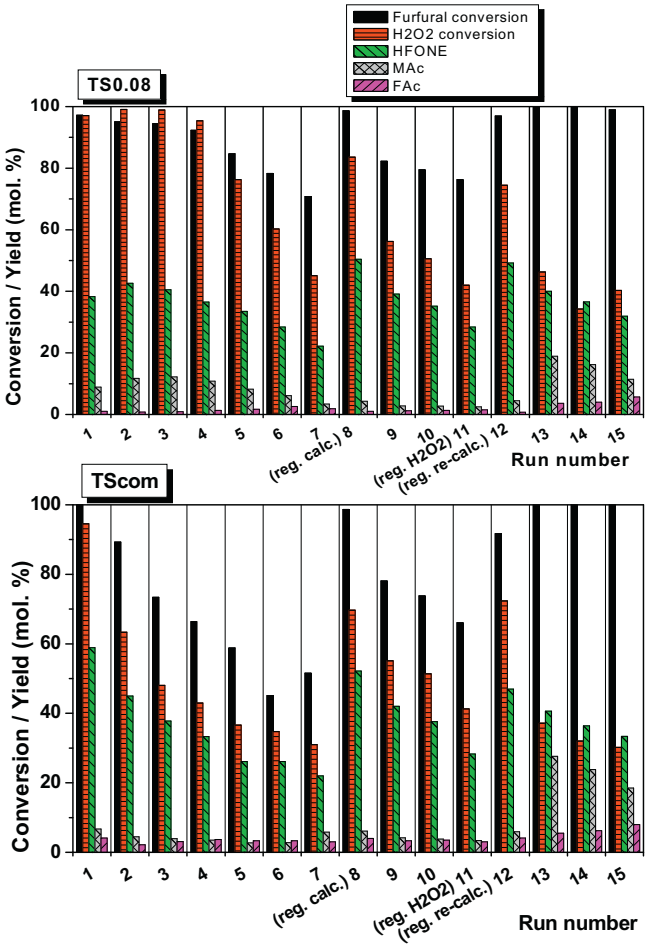

Fig. 8. Reutilization studies of TS0.08 catalyst and TScom (commercial catalyst) at 4 h of reaction time, 323 K, 5 wt.% of catalyst, 5 wt% of furfural and H_2O_2/FUR mol ratio of 2.5 (for the 13th, 14th and 15th runs, the H_2O_2/FUR mol ratio = 7.5).

3.3. Deactivation studies

The as-prepared TS-0.08 sample was subjected to a long series of successive catalytic runs. The reaction solutions after conducting these consecutive runs were also analysed to monitor the leaching of Ti [9]. Additionally the used catalyst was characterized by several techniques to examine the different Ti species present in the used catalyst. This sample was selected because it presented the largest incorporation of Ti to the silicalite framework, but it also had the largest concentration of extraframework Ti oxide. The study was conducted in a parallel manner on a commercial TS-1 catalyst used in a previous investigation (TScom) [9].

The reutilization results for TS0.08 and TScom (commercial catalysts) are presented in Fig. 8. The same reaction conditions selected for Figs. 5 and 7 were selected for runs 1–12. With this low H_2O_2/FUR ratio and short reaction time, the reaction is not complete and is more sensitive to deactivation processes. After the 7th run, the sample was taken out of the reactor and subjected to a calcination step using the same procedure used for calcining the fresh samples. Once calcined, the 8th run, named "reg. cal.", was conducted. Previously the calcined sample was weighed (loss of catalyst is unavoidable due to the handling needed for the calcination step, around 5% of catalyst was lost) and the amount of H_2O, furfural and H_2O_2 adjusted to maintain the same reaction conditions used for previous runs. The 11th run (called reg. H2O2) was conducted after attempting to regenerate the sample by using concentrated aqueous H_2O_2 solution (30 v/v%) at 323 K. The 12th

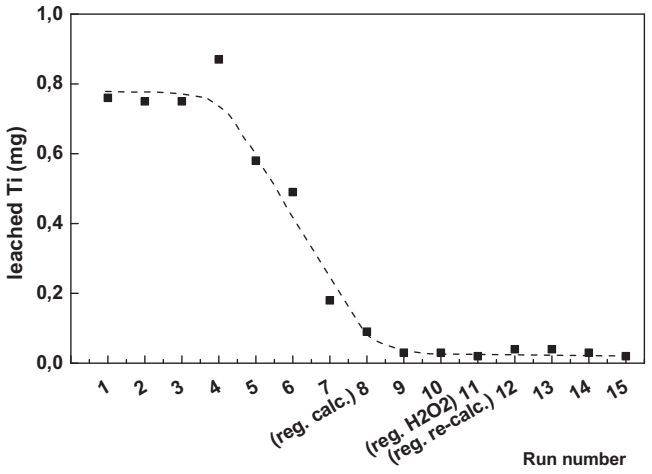

Fig. 9. Amount of Ti leached to the reaction mixture in successive runs expressed as mg of TiO_2 and analysed by TXRF.

run (reg. re-calc.) was conducted after regeneration by calcining again the previous used sample. The 13th, 14th and 15th runs were conducted with a H_2O_2/FUR mol ratio = 7.5.

Previous studies on TScom were conducted at 24 h of reaction [9] and no extensive deactivation processes were revealed. Now the conversion of furfural and H_2O_2 and yield of HFONE, MAc and FAc decreased upon reutilization. The deactivation rate is apparently faster for the commercial catalyst, but it is also evident in the TS0.08 catalyst beyond the 4th run. The calcination of the used samples after conducting the 7th run results in a remarkable regeneration of the catalyst (8th run). Actually in the case of the TS0.08 sample, the conversion of furfural and the yield of HFONE obtained in the 8th run are larger than for the 1st run, we will explain this effect later. This reactivation by calcination evidences that the catalysts have been deactivated by the deposition of carbonaceous species formed as minor by-products of the reaction. This deposits results in the fouling and/or poisoning of the active sites. They are removed by combustion in the calcination step. These species cannot be removed by aqueous oxidation with concentrated H_2O_2 as shown in the 11th run, but could be again removed by calcination (12th run) and consequently the catalyst substantially rejuvenated. The accumulation of these species is not related with the low H_2O_2/FUR ratio used, because deactivation is also observed when the reaction is conducted at higher H_2O_2 concentration like in the 13th, 14th and 15th runs (with H_2O_2/FUR mol ratio = 7.5). In these runs, the MAc yield was larger because the much higher H_2O_2 concentration accelerated the formation of MAc, but both the yields of HFONE and MAc decrease upon reusing the catalysts.

Finally another interesting effect can be noticed in the yield of MAc during the reusing of TS0.08 sample. Conversion of furfural and HFONE yield are remarkably recovered by calcination but MAc yield is not. Thus the MAc yield of the 8th run is smaller than that observed in the 1st run, MAc yield of the 9th run is smaller than that of the 2nd run, and so on. This effect will be explained below once the data of leaching of Ti during reusing have been discussed.

Fig. 9 presents the amount of Ti leached out to the aqueous reaction mixture (TXRF analysis) for the different runs conducted with the TS0.08 catalyst (expressed as mg of Ti). The figure clearly shows that Ti is being leached out during the reusing experiments. It must be taken into account that Ti oxide can be converted to soluble titanium peroxide species in the presence of H_2O_2. The leaching is intense (0.75–0.9 mg of TiO_2) for the first 4 runs, the reaction mixture for these first 4th runs presented an intense orange-yellow color indicating that soluble Ti-peroxo complexes were present in solution. In successive runs, the leaching becomes less intense

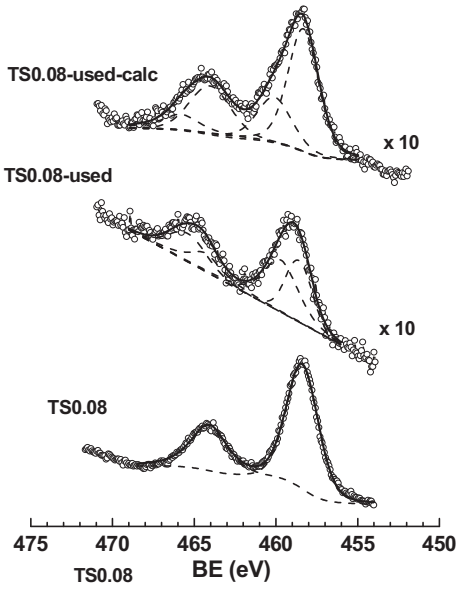

Fig. 10. Ti 2p core level of TS0.08, TS0.08-used and TS-0.08-used-calc samples.

and the color of the reaction mixtures turns into very pale yellow. Beyond the 8th run the leaching remains below 0.04 mg. The overall Ti loss by leaching measured in the liquids represented around 33% of the initial Ti loading. A similar behavior has been reported for the TScom catalyst in previous investigation [9].

Analysis of the catalytic and leaching data strongly suggests that, beside the deposition of by-products, the leaching of Ti is also deactivating the catalyst at a longer term but unfortunately in an irreversible manner. This behaviour is evident when comparing, one by one, the different cycles obtained after regeneration by calcination. Although the furfural conversion and HFONE yield obtained in 8th run (the first cycle after the first calcination step) are larger than those obtained with the fresh catalyst (1st run) for reasons that will be explain at the end of this section, the catalytic properties obtained in the 9th, 10th, 11th and 12th runs are slightly but visibly worse than in, respectively, the 2nd, 3rd, and 4th run. And those of 13th run (after a new calcination) are worse than those of 8th run. The same conclusion can be reached from the series of runs conducted with TScom. This difference cannot be due to the loss of catalyst during handling the catalyst, because after calcination the catalyst is weighed and the amount of H_2O, furfural and H_2O_2 used for the successive runs adjusted to take into account the losses of catalyst during handling and transfer and to maintain the same reaction conditions used for previous runs.

The Fig. 10 presents the Ti 2p XPS core level analysis of the used TS0.08 catalyst (TS0.08-used). For the sake of comparison the spectrum of the fresh (as-prepared) TS0.08 sample was also included. The used catalyst corresponds to that after the 15th runs in Fig. 8, collected from the reactor and subjected to five deionised water washing and centrifugation steps and finally dried at 333 K overnight. The Fig. 10 also includes the Ti 2p core level of this used sample after being calcined at 823 K (TS0.08-used-calc). A simple comparison of the intensity of the TS0.08-used sample with that of as-prepared TS0.08 indicates that the Ti concentration at the surface is ca. 10 times smaller (see the magnification factor of the used catalysts). Specifically, the XPS Ti/Si ratios of the fresh and used samples are 0.301 and 0.025, respectively (see Tables 1 and 2), representing a Ti loss of around 90%. According to the TXRF analysis of the liquid reaction mixtures, ca. 33% of Ti was lost during the 15 runs (quite similar values were obtained when comparing TXRF analyses of the fresh and used catalyst in Tables 1 and 2). These results indicate that the leaching of Ti is quite intense at the surface of the Ti-silicalite particles. A more careful inspection to the XPS spectra indicates that the leaching has mainly affected the octahedral Ti, because in the fresh TS0.08 sample its presence dominates the spectrum, while in the TS0.08-used spectrum both tetrahedral framework Ti and octahedral anatase Ti are visible. Consequently the XPS Ti/Si ratio for octahedral species decreases from 0.301 for fresh TS0.08 to 0.011 for TS0.08-used. Similar behaviour was observed for the TScom catalyst: overall XPS Ti/Si ratio decreases from 0.054 for fresh TScom to 0.023 for used TScom and the octahedral Ti/Si ratio from 0.015 to 0.001, respectively [9].

It is also worth noting that the total leaching along the 15th runs is as intense, as that obtained by washing with aqueous HCl (even more intense). This behaviour is evident by comparing both the TXRF and XPS Ti/Si ratio obtained from TS0.08-HCl and TS-0.08-used samples. Thus according to Table 2, the TXRF ratios are 0.047 and 0.033, respectively, and the XPS ratios are 0.137 and 0.025, respectively. It must also be noticed that the tetrahedral Ti/Si ratio in the TS0.08-used sample is also smaller than that found in the TS0.08-HCl sample (0.014 vs. 0.032), evidencing that the accumulated leaching during successive runs also affects the active framework Ti species. Finally the XPS analysis of the TS0.08-used-calc sample is in agreement with all the previous conclusions addressing the intense removal of Ti from the surface, especially the octahedral Ti but also of framework Ti species.

The TXRF and XPS results obtained in the reutilization studies give an explanation of why in the as-prepared TS0.08 sample the furfural conversion and HFONE yield obtained for the 8th run (after regeneration by calcination) are better than those obtained for the first run. The intense accumulated leaching of Ti species occurring during the first 7th cycles results in a substantial removal of the Ti oxide originally present in the fresh sample. It seems reasonable to assume that the Ti oxide nanodomains occluded within the channels and cages are substantially removed during these initial runs. Actually the DRIFT spectrum of acetonitrile obtained for the TS0.08-used (Fig. 6) shows that Lewis Ti(IV) sites are accessible to acetonitrile. In the 8th run, after the calcination step, reactants apparently have no restriction to the access to the active sites, because both occluded Ti oxide nanodomains and deposits of by-products have been removed. Consequenlty the catalytic properties are better than those obtained in the 1st run. A secondary beneficial effect of the leaching of Ti is the removal of the species responsible for the unselective conversion of H_2O_2, therefore the conversion of H_2O_2 in the 8th run is lower than on the 1st run.

To explain why the yield of MAc is not recovered after the calcination step (as mentioned above) it can be proposed that the occluded Ti oxide nanodomains are more active in the step of oxidation of HFONE to MAc than the tetrahedral Ti sites. At the 8th run, the former species have extensively been removed by leaching during the previous runs and therefore they are not anymore available to catalyze this step. Something similar may have occurred when washing the TS0.04 and TS0.08 samples with HCl. The MAc yield of the HCl-washed samples is lower than that of the as-prepared samples presumably because the occluded Ti oxide nanodomains have been removed.

4. Conclusions

Two types of extraframework Ti have been identified: (i) anatase Ti oxide located at the external surface of zeolite crystals and (ii) Ti oxide nanodomains occluded within the channels and cavities of the zeolite. Both extraframework Ti species can be responsible of the unselective consumption of H_2O_2. When the occluded Ti oxide nanodomains are at high concentration, they can restrict the access of the reactants to the effective active sites (the tetrahedral Ti incorporated to the silicalite framework). This results in

lower yield of the oxidation products than expected considering the amount of active Ti(IV) sites that have been incorporated to the framework. These blocking Ti oxide nanodomains can be removed by a previous HCl-washing step. However it must be noticed that this rinsing step is not really needed because they are also removed during the progress of the reaction runs as they are solubilized by the formation of soluble Ti-peroxo complexes.

The deposition of reaction by-products is the main short term source of deactivation, but the activity can be significantly recovered by removing these deposits by calcination at 573 K under air. Both the extraframework Ti and the framework Ti are leached into the reaction mixture during the course of the reaction. Leaching of the latter irreversibly deactivates the catalyst in the long term.

Acknowledgments

Financial support from the Spanish Ministry of Economy and Competitiveness is gratefully acknowledged (project CTQ2012-38204-C03-01). M.L.G also thanks the Ministery of Education, Culture and Sports for a "Salvador de Madariaga" grant (PRX14/00234) and CSIC for financial support from i-link project (i-link1048). The authors acknowledge the use of facilities and instrumentation supported by the University of Wisconsin Materials Research Science and Engineering Center (grant DMR-1121288).

Appendix A. Supplementary data

Supplementary data associated with this article can be found, in the online version, at http://dx.doi.org/10.1016/j.apcatb.2016.09.025.

References

[1] J.C.B., T.R. Felthouse, B. Horrell, M.J. Mummey, Yeong-Jen Kuo, Kirk-Othmer Encyclopedia of Chemical Technology Online, 2001.
[2] H.H.K. Lohbeck, W. Fuhrmann, N. Fedtke, Ullmannís Encyclopedia of Industrial Chemistry, Weinheim, Germany (2000), 463–473.
[3] G. Pavarelli, J. Velasquez Ochoa, A. Caldarelli, F. Puzzo, F. Cavani, J.L. Dubois, ChemSusChem 8 (2015) 2250–2259.
[4] A. Chatzidimitriou, J.Q. Bond, Green Chem. 17 (2015) 4367–4376.
[5] X. Li, Y. Zhang, Green Chem. 18 (2016) 643–647.
[6] N. Alonso-Fagúndez, M. López Granados, R. Mariscal, M. Ojeda, ChemSusChem 5 (2012) 1984–1990.
[7] H. Guo, G. Yin, J. Phys. Chem. C 115 (2011) 17516–17522.
[8] S. Shi, H. Guo, G. Yin, Catal. Commun. 12 (2011) 731–733.
[9] N. Alonso-Fagundez, I. Agirrezabal-Telleria, P.L. Arias, J.L.G. Fierro, R. Mariscal, M.L. Granados, RSC Adv. 4 (2014) 54960–54972.
[10] J. Lan, Z. Chen, J. Lin, G. Yin, Green Chem. 16 (2014) 4351–4358.
[11] H. Choudhary, S. Nishimura, K. Ebitani, Appl. Catal. A-Gen. 458 (2013) 55–62.
[12] H. Choudhary, S. Nishimura, K. Ebitani, Chem. Lett. 41 (2012) 409–411.
[13] X. Li, B. Ho, Y. Zhang, Green Chem. 18 (2016) 2976–2980.
[14] A.S. Mamman, J.M. Lee, Y.C. Kim, I.T. Hwang, N.J. Park, Y.K. Hwang, J.S. Chang, J.S. Hwang, Biofuels Bioprod. Biorefin. 2 (2008) 438–454.
[15] R. Karinen, K. Vilonen, M. Niemelä, ChemSusChem 4 (2016) 1002–1016.
[16] K.J. Zeitsch, The Chemistry and Technology of Furfural and Its Many By-Products, Sugar Series, vol. 13, Elsevier, The Netherlands, 2000.
[17] R. Mariscal, P. Maireles-Torres, M. Ojeda, I. Sádaba, M. López Granados, Energy Environ. Sci. 9 (2016) 1144–1189.
[18] J.S. Luterbacher, D. Martin Alonso, J.A. Dumesic, Green Chem. 16 (2014) 4816–4838.
[19] J.J. Bozell, G.R. Petersen, Green Chem. 12 (2010) 539–554.
[20] J. Wahlen, B. Moens, D.E. De Vos, P.L. Alsters, P.A. Jacobs, Adv. Synth. Catal. 346 (2004) 333–338.
[21] P. Kumar, R.K. Pandey, Green Chem. 2 (2000) 29–31.
[22] G.N. Vayssilov, Catal. Rev. Sci.-Eng. 39 (1997) 209–251.
[23] C. Liu, J. Huang, D. Sun, Y. Zhou, X. Jing, M. Du, H. Wang, Q. Li, Appl. Catal. A 459 (2016) 1–7.
[24] R. Millini, E. Previde Massara, G. Perego, G. Bellussi, J. Catal. 137 (1992) 497–503.
[25] M.A. Uguina, D.P. Serrano, R. Sanz, J.L.G. Fierro, M. López-Granados, R. Mariscal, Catal. Today 61 (2000) 263–270.
[26] Q. Wang, L. Wang, J. Chen, Y. Wu, Z. Mi, J. Mol. Catal. A-Chem. 273 (2007) 73–80.
[27] X. Zhang, Y. Wang, F. Xin, App. Catal. A-Gen. 307 (2006) 222–230.
[28] I. Sádaba, M. López Granados, A. Riisager, E. Taarning, Green Chem. 17 (2015) 4133–4145.
[29] A.J.H.P. van der Pol, J.H.C. van Hooff, Appl. Catal. A Gen. 92 (1992) 93–111.
[30] H.M. Rietveld, J. Appl. Crystallogr. 2 (1969) 65–71.
[31] A.C.L.a.R.B.V. Dreele, Los Alamos National Laboratory Report LAUR 86–748.
[32] C.D. Wagner, J. Electron Spectrosc. 32 (1983) 99–102.
[33] T. Armaroli, F. Milella, B. Notari, R.J. Willey, G. Busca, Top. Catal. 15 (2001) 63–71.
[34] C. Lamberti, S. Bordiga, A. Zecchina, A. Carati, A.N. Fitch, G. Artioli, G. Petrini, M. Salvalaggio, G.L. Marra, J. Catal. 183 (1999) 222–231.
[35] N. Alonso-Fagúndez, V. Laserna, A.C. Alba-Rubio, M. Mengibar, A. Heras, R. Mariscal, M.L. Granados, Catal. Today (2014).
[36] J. Mühlebach, K. Müller, G. Schwarzenbach, Inorg. Chem. 9 (1970) 2381–2390.
[37] M. Kakihana, M. Kobayashi, K. Tomita, V. Petrykin, Bull. Chem. Soc. Jpn. 83 (2010) 1285–1308.
[38] A.A. Baba, F.A. Adekola, E.E. Toye, R.B. Bale, J. Miner. Mater. Charact. Eng. 08 (10) (2009) 15.
[39] F. Bonino, A. Damin, S. Bordiga, C. Lamberti, A. Zecchina, Langmuir 19 (2003) 2155–2161.
[40] R. Mariscal, M. López-Granados, J.L.G. Fierro, J.L. Sotelo, C. Martos, R. Van Grieken, Langmuir 16 (2000) 9460–9467.
[41] M. Tamura, W. Chaikittisilp, T. Yokoi, T. Okubo, Microporous Mesoporous Mater. 112 (2008) 202–210.

Update

Applied Catalysis B: Environmental
Volume 238, Issue , 15 December 2018, Page 672

DOI: https://doi.org/10.1016/j.apcatb.2017.02.006

Applied Catalysis B: Environmental 238 (2018) 672

Contents lists available at ScienceDirect

Applied Catalysis B: Environmental

journal homepage: www.elsevier.com/locate/apcatb

Corrigendum

Corrigendum to "Oxidation of furfural in aqueous H_2O_2 catalysed by titanium silicalite: Deactivation processes and role of extraframework Ti oxides" [Appl. Catal. B: Environ. 202 (2017) 269–280]

A.C. Alba-Rubio[a,1], J.L.G. Fierro[b], L. León-Reina[c], R. Mariscal[b], J.A. Dumesic[a], M. López Granados[b,*]

[a] Department of Chemical and Biological Engineering, University of Wisconsin-Madison, 1415 Engineering Drive, Madison, WI, United States
[b] Instituto de Catálisis y Petroleoquímica (CSIC), C/Marie Curie, Campus de Cantoblanco, E-28049 Madrid, Spain
[c] Servicios Centrales de Apoyo a la Investigación, SCAI, Universidad de Málaga, Campus Teatinos s/n, 29071 Málaga, Spain

The authors regret to inform that there were some mistakes in the description of the temperature and protocol for the calcination of fresh and used samples. Samples were always calcined at 823 K. Consequently the following sentences must be corrected:

- In the abstract the sentence "The former can be reverted by removal of the deposits through calcination under air at 773 K." must be substituted by the sentence "The former can be reverted by removal of the deposits through calcination under air at **823** K."
- In the section 2.1 the sentence "The solid was then dried at 393 K for 2 h (heating ramp 0.030 K min^{-1}) and then calcined at 623 K for 10 h (heating ramp 0.083 K min^{-1})." must be replaced by the sentence "The solid was then dried at 393 K for 2 h (heating ramp **0.033 K** $\mathbf{s^{-1}}$) and then calcined at **823** K for 10 h (heating ramp **0.083 K** $\mathbf{s^{-1}}$)."
- In the section 2.2, when describing the recording of Raman spectra, the sentence "Raman spectra were recorded at room temperature with a laser power of 2 mW after an in situ calcination of the samples in synthetic air with a heating rate of 10 K min^{-1} up to 833 K for 30 min." must be replaced by "Raman spectra were recorded at room temperature with a laser power of 2 mW after an in situ calcination of the samples in synthetic air with a heating rate of **0.17 K** $\mathbf{s^{-1}}$ up to **823** K for 30 min."
- In the last paragraph of the Conclusions sections the sentence "The deposition of reaction by-products is the main short term source of deactivation, but the activity can be significantly recovered by removing these deposits by calcination at 573 K under air." must be replaced by "The deposition of reaction by-products is the main short term source of deactivation, but the activity can be significantly recovered by removing these deposits by calcination at **823** K under air."

The authors would like to apologise for any inconvenience caused.

DOI of original article: http://dx.doi.org/10.1016/j.apcatb.2016.09.025.
* Corresponding author.
E-mail address: mlgranados@icp.csic.es (M.L. Granados).
[1] Present address: Department of Chemical and Environmental Engineering, University of Toledo, Toledo, OH 43606, United States.

https://doi.org/10.1016/j.apcatb.2017.02.006
0926-3373/